THRESHOLD-FREE ADAPTIVE OPEN-SET CLASSIFIER FOR SAR TARGET RECOGNITION

Yue Li[1], Haohao Ren[1*], Xuelian Yu[1], Chengfa Zhang[2], Lin Zou[1], Yun Zhou[1]

[1] University of Electronic Science and Technology of China, Chengdu 611731, China
[2] Chengdu Lingjie Technology Corporation, Chengdu 8092, China
** haohao_ren@uestc.edu.cn*

Keywords: SYNTHETIC APERTURE RADAR, AUTOMATIC TARGET RECOGNITION, GENERATIVE ADVERSARIAL NETWORK, OPEN SET RECOGNITION

Abstract

Many synthetic aperture radar (SAR) automatic target recognition (ATR) techniques are constrained by the closed-set environment assumption, resulting in a failure to detect targets from novel categories. To address the challenges of SAR ATR in an open world, we propose a threshold-free adaptive open-set classifier (TfAOsC) for SAR open set recognition (OSR). With the help of generative adversarial network (GAN), the proposed TfAOsC adaptively transforms the OSR task into a K+1-way classification problem, achieving both known class classification and unknown class identification without a predefined threshold. First, to generate diverse SAR images of unknown classes, Kullback–Leibler (KL) divergence is leveraged to enlarge the difference between generated image pairs sharing the same label. Moreover, we design a multi-task optimization loss to enhance the recognition performance of the proposed method. Experimental results on moving and stationary target acquisition (MSTAR) and synthetic and measured paired and labeled experiment (SAMPLE) datasets demonstrate the effectiveness of the proposed method over some state-of-the-art open-set SAR target recognition approaches.

1 Introduction

Synthetic aperture radar (SAR) plays a major role in the fields of remote sensing, surveillance, and guidance due to its high resolution in all-day and all-weather conditions. In order to interpret SAR imagery efficiently and accurately, automatic target recognition (ATR) for SAR targets has become one of the most popular research areas.

With the rapid advancement of machine learning and deep neural network (DNN), several DNN-based ATR methods for SAR imagery have been proposed in recent years. For instance, Chen *et al.* [1] devised an all-convolutional classification network for SAR target recognition. Ren *et al.* presented a convolutional capsule network to achieve robust SAR ATR performance under extended operation conditions [2]. Pei *et al.* [3] proposed a multi-view SAR ATR approach using a parallel convolutional neural network. However, most of these methods assume a closed set environment, which means they do not consider the presence of novel classes of targets during the reasoning process. This could lead to important information being missed and misclassified, making it challenging to adapt to real-world scenarios.

To tackle this problem, Scheirer *et al.* introduced open set recognition (OSR) [4] paradigm, which requires models that not only accurately classify known classes, but also effectively identify unknown classes. Bendale and Boult first presented an openmax (OpenMax) classifier [5] based on deep learning (DL) techniques to identify unknown images. Chen *et al.* proposed an open-set recognition strategy called adversarial reciprocal point learning (ARPL) to learn unknown distribution [6]. In the past decade, several researchers have also proposed OSR methods for SAR targets. For example, Giusti *et al.* [7] introduced the OpenMax classifier to achieve known class classification and unknown class identification for SAR targets. Ma *et al.* developed a multitask learning framework based on conditional generative adversarial network (CGAN) for open-set SAR target recognition [8]. Safaei *et al.* [9] proposed a category-aware binary classifier (CBC) module to learn the decision boundary for each category and thus achieve open-set classification. However, existing open-set SAR target recognition methods rely heavily on a predefined threshold to identify targets of unknown classes, which limits the adaptability and flexibility of these models.

Therefore, to move away from making decisions based on empirical knowledge, this paper proposes a threshold-free adaptive open-set classifier (TfAOsC) for open-set SAR target recognition. With the help of generative adversarial network (GAN) framework, we adaptively transform the open-set SAR target recognition task into a K+1-way classification problem. Specifically, to avoid model collapse of the generator, we leverage KL divergence to enlarge the difference between generated image pairs sharing the same label, aiming to enrich the diversity of generated unknown classes. Furthermore, we design a multi-task optimization loss to enhance the generalization ability and overall recognition performance of the proposed method.

The remainder of the paper is organized as follows. In Section 2, we introduce the proposed TfAOsC method in detail. In Section 3, we address the dataset description, the experimental setup, and the performance results on two public SAR imagery datasets. Finally, the conclusion is drawn in Section 4.

2 Methodology

The overall framework of the proposed TfAOsC is shown in Fig. 1, which is composed of two key components: the generator *G* and the discriminator *D*. The network structure of *G* and *D* is illustrated in Fig. 2. Among them, the generator *G* is used to learn the distribution of known SAR images and generate unknown samples, thereby providing the discriminator *D* with extra unknown information that enables it to adaptively detect targets from unknown classes.

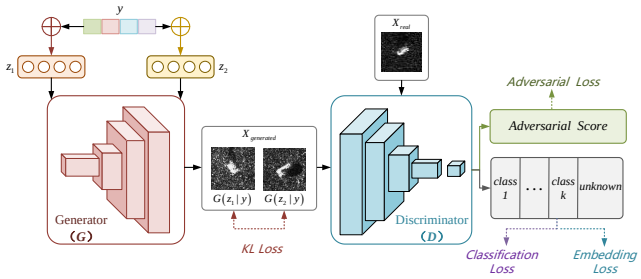

Fig. 1. Overall framework of the proposed method.

2.1 Generating Diverse Unknown Images

Different from closed-set scenarios, SAR ATR models have no prior information about unknown classes in an open world, which poses challenges in tackling open-set recognition tasks. To address this problem, we leverage a generative model to generate unknown SAR images close to real images, enabling the discriminator to effectively detect unknown targets. Specifically, with the help of GAN model, we adaptively transform the open-set SAR target recognition task into a *K*+1-way classification problem. To generate diverse unknown samples and provide the discriminator with effective unknown information, we propose to synthesize image pairs by two noise inputs sharing the same label. Then, KL divergence is utilized to maximize the difference between corresponding generated images, which can be written as Eq. (1). This can further prevent the model collapse of the generator, as *G* is penalized when it outputs overly similar images.

$$\max KL[G(z_1|\ y)\,||\,G(z_2|\ y)] \tag{1}$$

where z_1 and z_2 represent two random noise vectors given the same class label y. Correspondingly, $G(z_1|\ y)$ and $G(z_2|\ y)$ denote generated unknown SAR images. KL divergence is leveraged to maximize the difference between these image pairs.

2.2 Adaptive Open-set Classifier

In order to effectively achieve known class classification and unknown class identification, we propose an adaptive open-set classifier based on GAN model. As shown in Fig. 2(b), the discriminator *D* can directly work as a *K*+1-way classifier under the open-set environment. There are two output branches of *D*: the scoring branch and the classification branch. Among them, the scoring branch gives a confidence score

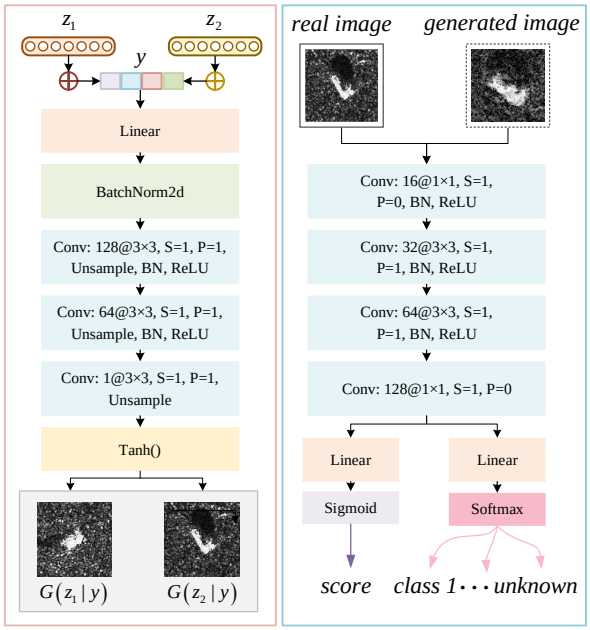

(a) (b)

Fig. 2. Network structure of (a) Generator, (b) Discriminator. Conv denotes a convolution layer. *c* @ *k* × *k*, *S* = *s*, *P* = *p* indicates the layer contains *c* output channels and the kernel size of *k*×*k* convolution with stride = *s* and padding = *p*.

ranging from 0 to 1, with a value closer to 1 indicating a more realistic SAR image. And the classification branch outputs probability for *K*+1 classes and corresponding class label.

2.3 Multi-task Loss Optimization

The training procedure of GAN model is performed in an adversarial manner between generator *G* and discriminator *D*, which is also known as a minimax game [10]. The adversarial loss of *G* and *D* are defined in Eq. (2) and Eq. (3):

$$l_{G\_adv} = -E\left[\log P(S = unknown \mid X_{unknown})\right] \tag{2}$$

$$l_{D\_adv} = E\left[\log P(S = real \mid X_{real})\right] \tag{3}$$

where X_{real} and $X_{unknown}$ denote real SAR images and generated ones, respectively. And $P(S \mid X)$ represents the probability of a given image input being real.

On the other hand, aiming to generate unknown images that assist the open-set classifier in addressing known class classification and unknown class recognition tasks, the classification loss is shown in the following equations:

$$l_{G\_cls} = E\left[\log P\left(C = c \middle| X_{unknown}\right)\right] \tag{4}$$

$$\begin{aligned} l_{D\_cls} &= E\left[\log P\left(C = c \middle| X_{real}\right)\right] \\ &+ E\left[\log P\left(C = unknown \middle| X_{unknown}\right)\right] \end{aligned} \tag{5}$$

where c is the class label of one of the K known classes.

In order to enhance the generalization ability of our proposed method, we use soft labels instead of one-hot labels for model training, as expressed in Eq. (6). Thus, l_{D_cls} is the label smoothing cross-entropy loss function, which improves the overall recognition performance by increasing the known classes classification accuracy [11]. The soft label of a sample is defined as:

$$y = (1-\alpha)\, y_{hot} + \frac{\alpha}{K} \tag{6}$$

where y_{hot} denotes the one-hot label of an image, α is the smoothing parameter, and K is the number of known classes.

As previously mentioned, we use KL divergence to generate diverse SAR images of unknown class and avoid the model collapse of the generator, which is written as KL loss:

$$l_{G\_kl} = -KL[G(z_1 | y) \,||\, G(z_2 | y)] \tag{7}$$

As we can see from Fig. 2(b), the discriminator network is employed to extract feature representations of real and generated SAR images. In order to obtain an open-set embedding space with intra-class compactness and inter-class separability to further enhance the open-set recognition performance of our proposed TfAOsC, single-center loss (SCL) [12] is introduced to learn a discriminative embedding representation space. The embedding loss is shown as:

$$l_{D\_emb} = M_{real} - M_{unknown} + m\sqrt{N} \tag{8}$$

where M_{real} and $M_{unknown}$ represent the mean Euclidean distance from representations of real SAR images and generated ones to the centroid of known classes targets, respectively. The margin item $m\sqrt{N}$ is added to ensure that $M_{unknown}$ is greater than M_{real}, thereby the embedding loss can remain positive, and can be propagated effectively.

The equations of M_{real} and $M_{unknown}$ are expressed as follows:

$$M_{real} = \frac{1}{|S_{real}|} \sum\nolimits_{i \in S_{real}} \| f_i - C \|_2 \tag{9}$$

$$M_{unknown} = \frac{1}{|S_{unknown}|} \sum\nolimits_{i \in S_{unknown}} \| f_i - C \|_2 \tag{10}$$

where S_{real} and $S_{unknown}$ are the representation sets of real SAR images and generated ones, respectively. f_i denotes the feature representation of a given sample i, and C is the centroid representation of known classes targets.

To sum up, the proposed multi-task loss functions are comprised of three parts: adversarial loss, classification loss and optimization loss. The total loss for the generator *G* and the discriminator *D* can be written as:

$$l_G = l_{G\_adv} + l_{G\_cls} + \lambda_G \times l_{G\_kl} \tag{11}$$

$$l_D = l_{D\_adv} + l_{D\_cls} + \lambda_D \times l_{D\_emb} \tag{12}$$

where λ_G and λ_D are two weight hyperparameters.

3 Experimental Results

3.1 Data Description

To validate the performance of the proposed method, this section conducts a series of experiments on two public SAR datasets: the moving and stationary target acquisition and recognition (MSTAR) [13] dataset and the synthetic and measured paired and labeled experiment (SAMPLE) [14] dataset. The MSTAR dataset is provided by the U.S. Defense Advanced Research Projects Agency (DARPA), which contains 10 classes of military vehicles. The SAMPLE dataset is composed of measured images from the MSTAR dataset and simulated images with 10 classes of ground targets. We show the detailed information of MSTAR and SAMPLE in Table 1. Following previous studies [2], [3], [8], we use SAR images at a depression angle of 17° as the train set and images at 15° as the test data in the MSTAR dataset. In the SAMPLE dataset, only measured SAR images with depression from 14° to 16° are selected for training, and images with 17° depression are used for testing. All the SAR images are cropped to the size of 64×64 pixels regions of interest.

Table 1 Detailed Information of MSTAR and SAMPLE

MSTAR			SAMPLE		
Target	Train	Test	Target	Train	Test
2S1	299	274	2S1	116	58
BMP2	233	195	BMP2	55	52
BRDM2	298	274	BTR70	43	49
BTR60	256	195	M1	78	51
BTR70	233	196	M2	75	53
D7	299	274	M35	76	53
T62	299	273	M548	75	53
T72	232	196	M60	116	60
ZIL131	299	274	T72	56	52
ZSU23/4	299	274	ZSU23	116	58
Total	2747	2425	**Total**	806	539

3.2 Experimental Setup

The proposed method is performed on a personal laptop with an AMD Ryzen 7 5800H CPU, an NVIDIA GeForce RTX3060 GPU, and 16 GB memory. Adam is used for optimizing the proposed model and the learning rate for both the generator and the discriminator is set as 0.00005. For the four hyperparameters, we set $\alpha = 0.1$, $m = 0.3$, $\lambda_G = 0.5$ and $\lambda_D = 0.1$ in the following experiments.

Table 2 Four Evaluation Metrics of Each Method on The MSTAR and SAMPLE Datasets

Dataset	MSTAR				SAMPLE			
Method	Precision	Recall	F1-score	Accuracy	Precision	Recall	F1-score	Accuracy
OpenMax [5]	86.80	69.71	0.7429	69.60	87.40	83.21	0.8440	80.80
ARPL [6]	83.39	87.90	0.8595	85.81	88.44	90.81	0.8916	87.38
Mutitask Learning [8]	92.97	84.94	0.8823	86.35	90.47	92.65	0.9101	90.20
CBC [9]	91.69	86.72	0.8827	86.31	93.37	93.40	0.9316	91.28
Ours	**93.40**	**92.11**	**0.9232**	**91.67**	**95.62**	**94.72**	**0.9505**	**95.60**

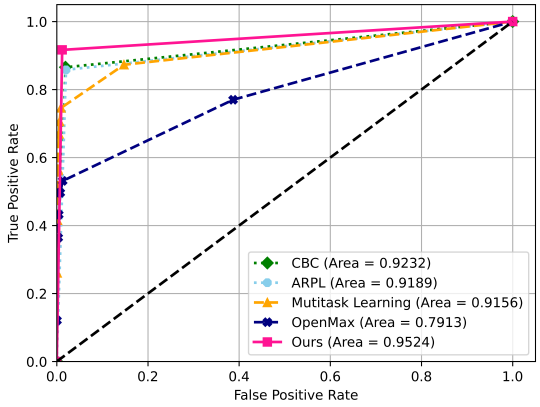

Fig. 3. Comparisons of AUROC on the MSTAR dataset.

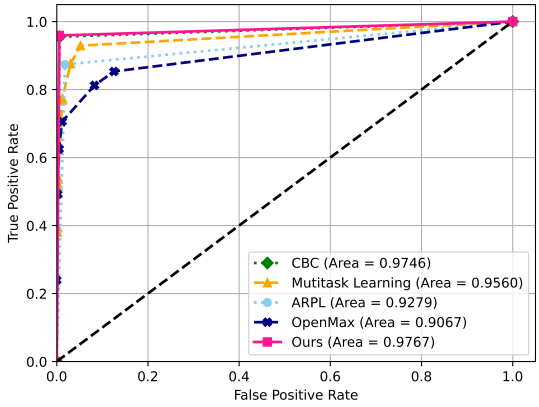

Fig. 4. Comparisons of AUROC on the SAMPLE dataset.

3.3 OSR Performance Evaluation

Following the experimental setting described in [9], we select 7 classes of SAR images as known targets to train the open-set ATR model. Specifically, 2S1, BRDM2, BTR60, D7, T62, ZIL131, ZSU23/4 for the MSTAR dataset, and 2S1, BMP2, BTR70, M1, M35, M548, ZSU23 for SAMPLE dataset. To validate the effectiveness of our proposed method in open-set recognition problem, we compare it with four state-of-the-art OSR methods for SAR targets, namely, OpenMax [5], ARPL [6], Mutitask Learning [8], and CBC [9].

We employ four evaluation metrics, i.e., precision, recall, F1-score, and accuracy to comprehensively measure the open-set recognition performance of the proposed method. The experimental results are summarized in Table 2. Specifically, accuracy shows the average performance of known class classification and unknown class identification, and F1-score measures the overall OSR performance as it balances the trade-off between precision and recall. The results in Table 2 clearly demonstrate that TfAOsC outperforms all competitors on both datasets, with higher scores across four evaluation metrics.

Moreover, the area under ROC curve (AUROC) is another evaluation metric commonly used to measure the performance of OSR methods. In this experiment, we present the AUROC results for each method on two datasets, as depicted in Fig. 3 and Fig. 4, respectively. It is obvious that our TfAOsC also outperforms the other four methods in terms of AUROC.

3.4 Impact of openness on OSR

In order to assess the robustness of the proposed method under different ratios of known and unknown classes, the notion *openness* [4] is defined as:

$$openness = 1 - \sqrt{\frac{2\times|C_{TR}|}{|C_{TR}|+|C_{TE}|}} \tag{13}$$

where $|C_{TR}|$ is the number of training classes, and $|C_{TE}|$ is the number of testing classes. The closer *openness* to 1, the more open the environment is, while *openness* of 0 represents that the problem is equivalent to the closed-set classification.

In our experiment, we reduce the number of known classes from 7 to 3 with an interval of 1, and the corresponding *openness* increases from 9.25% to 32.06%. As illustrated in Fig. 5 and Fig. 6, we plot the F1-score and accuracy results of each method under different open scenarios on the MSTAR dataset and the SAMPLE dataset, respectively. Clearly, the performance curves of all the competitors show significant fluctuations with the increase of *openness* . In contrast, our proposed TfAOsC demonstrates superior robustness with various *openness* in the open world.

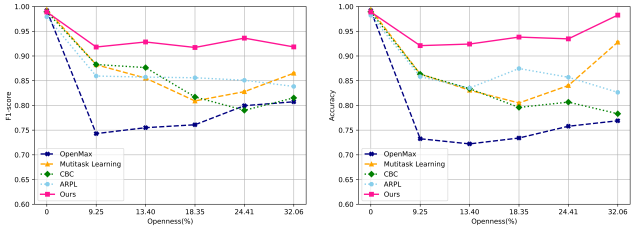

(a) (b)

Fig. 5. Results with various openness on the MSTAR dataset. (a) F1-score, (b) Accuracy.

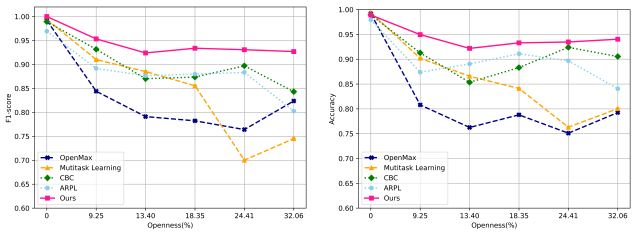

(a) (b)

Fig. 6. Results with various openness on the SAMPLE dataset. (a) F1-score, (b) Accuracy.

4 Conclusion

In this paper, we propose an adaptive open set classifier to solve the open-set recognition problem for SAR targets with the help of GAN framework. Unlike existing open-set SAR target recognition methods that rely on a predefined threshold to determine whether the target belongs to a novel class during the inference phase, we adaptively transform the open-set SAR target recognition task into a K+1-way classification problem. The proposed diverse sample generation strategy based on KL divergence can avoid the model collapse problem and thus improve the efficiency of training. The proposed multi-task optimization loss for both the generator and the discriminator further improves the overall recognition performance and generalization ability of the open-set method. Experimental results on two public SAR datasets demonstrate that the proposed TfAOsC outperforms four advanced open-set SAR target recognition methods.

5 Acknowledgement

This work was supported by the National Natural Science Foundation of China under Grants (No.62201124 and No.42027805).

6 References

[1] S. Chen, H. Wang, F. Xu, et al.: 'Target classification using the deep convolutional networks for SAR images', IEEE Trans. Geosci. Remote Sens., 2016, 54, (8), pp. 4806-4817.

[2] H. Ren, X. Yu, L. Zou, et al.: 'Extended convolutional capsule network with application on SAR automatic target recognition', Signal Process., 2021, 183, p. 108021.

[3] J. Pei, Y. Huang, W. Huo, et al.: 'SAR automatic target recognition based on multiview deep learning framework', IEEE Trans. Geosci. Remote Sens., 2017, 56, (4), pp. 2196–2210.

[4] W. J. Scheirer, A. de Rezende Rocha, A. Sapkota, et al.: 'Toward open set recognition', IEEE Trans Pattern Anal. Mach. Intell., 2013, 35, (7), pp. 1757–1772.

[5] A. Bendale and T. E. Boult.: 'Towards open set deep networks', in Proc. IEEE Conf. Comput. Vis. Pattern Recognit., 2016, pp. 1563-1572.

[6] G. Chen, P. Peng, X. Wang, et al.: 'Adversarial reciprocal points learning for open set recognition', IEEE Trans. Pattern Anal. Mach. Intell., 2021, 44, (11), pp. 8065–8081.

[7] E. Giusti, S. Ghio, A. H. Oveis, et al.: 'Open set recognition in synthetic aperture radar using the openmax classifier', in Proc. IEEE Radar Conf. (RadarConf), 2022, pp. 1–6.

[8] X. Ma, K. Ji, L. Zhang, et al.: 'An open set recognition method for SAR targets based on multitask learning', IEEE Geosci. Remote Sens. Lett., 2021, 19, pp. 1–5.

[9] B. Safaei, V. Vibashan, C. M. de Melo, et al.: 'Open-set automatic target recognition', in Proc. IEEE Int. Conf. Acoust., Speech Signal Process. (ICASSP), Rhodes Island, Greece, June. 2023, pp. 1–5.

[10] I. Goodfellow, J. Pouget-Abadie, M. Mirza, et al.: ' Generative adversarial nets', in Proc. Conf. Neural Inf. Process. Syst., Montreal, Canada, Dec. 2014, pp.2672-2680.

[11] S. Vaze, K. Han, A. Vedaldi, et al.: 'Open-set recognition: A good closed-set classifier is all you need', in Proc. Int. Conf. Learn. Representations, 2022.

[12] Li, H. Xie, J. Li, et al.: 'Frequency-aware discriminative feature learning supervised by single-center loss for face forgery detection', in Proc. IEEE/CVF Conf. Comput. Vis. Pattern Recognit., 2021, pp. 6458–6467.

[13] T. D. Ross, S. W. Worrell, V. J. Velten, et al.: 'Standard SAR ATR evaluation experiments using the MSTAR public release data set', in Proc. Algorithms Synth. Aperture Radar Imag., 1998, 3370, pp. 566-583.

[14] B. Lewis, T. Scarnati, E. Sudkamp, et al.: 'A SAR dataset for ATR development: the synthetic and measured paired labeled experiment (sample)', in Proc. Algorithms Synth. Aperture Radar Image., 2019, 10987, pp. 39-54.